[4]Hohenemser, K. H. and Yin, Shen-Kuang, "Some Applications of the Method of Multi-blade Coordinates," *Journals of the American Helicopter Society*, Vol. 17, No. 3, July 1972, pp. 3–12.

[5]Coleman, R. P., "Theory of Self-Excited Mechanical Oscillations of Hinged Rotor Blades," NACA Advanced Restricted Rept. 3G29, Republished as Rept. 1351, 1943, NACA.

[6]Miller, R. H., "Helicopter Control and Stability in Hovering Flight," *Journal of the Aeronautical Sciences*, Vol. 15, No. 8, Aug. 1948, pp. 453–472.

[7]Azuma, A., "Dynamic Analysis of the Rigid Rotor System," *Journal of Aircraft*, Vol. 4, No. 3, May-June 1967, pp. 203–209.

[8]Curtiss, H. C., Jr. and Shupe, N. K., "A Stability and Control Theory for Hingeless Rotors," American Helicopter 27th Annual National V/STOL Forum, Washington, D. C., May 1971.

[9]Ward, J. F., "Exploratory Flight Investigation and Analysis of Structural Loads Encountered By A Helicopter Hingeless Rotor System," D-3676, Nov. 1966, NASA.

[10]Harris, F. D., "Articulated Rotor Blade Flapping Motion at Low Advance Ration," *Journal of the American Helicopter Society*, Vol. 17, No. 1, Jan. 1972, pp. 41–48.

[11]Ormiston, R. A. and Peters, D. A., "Hingeless Helicopter Rotor Response with Nonuniform Inflow and Elastic Blade Bending," *Journal of Aircraft*, Vol. 9, No. 10, Oct. 1972, pp. 730–736.

MAY 1973 J. AIRCRAFT VOL. 10, NO. 5

Vortex Noise of Isolated Airfoils

Robert W. Paterson,* Paul G. Vogt,† Martin R. Fink‡
United Aircraft Research Laboratories, East Hartford, Conn.
and
C. Lee Munch§
Sikorsky Aircraft Division, Stratford, Conn.

An experimental study of airfoil vortex shedding noise in a low-turbulence flow and in a Reynolds number range applicable to full-scale helicopter rotors is described. Measurements of far-field noise, airfoil surface pressure fluctuations and correlation coefficients were obtained for NACA 0012 and NACA 0018 two-dimensional models and a finite-span NACA 0012 airfoil. Airfoil vortex shedding noise was found to be discrete rather than broadband, with the frequency predicted by a Strouhal number of approximately 0.1 referenced to twice the trailing-edge laminar boundary-layer thickness. At Reynolds numbers and angles of attack for which this boundary layer was turbulent on both surfaces, vortex shedding noise was undetectable. The effects of airfoil thickness change and finite airfoil span were found to be small, consistent with their influence on the pressure-surface laminar boundary layer. Cited examples of helicopter tail rotor, model propeller, sailplane flyby and low-Reynolds number isolated-airfoil data show that vortex shedding noise exists on these devices as a discrete-frequency phenomenon with the frequencies well predicted by the scaling law developed in the present study.

Introduction

HELICOPTER rotor and propeller noise spectra exhibit both a discrete-frequency and broadband character. The discrete-frequency or rotational noise is caused by steady and periodically fluctuating blade loads at frequencies which are integer multiples of blade rotative speed. The sources of broadband noise can be conveniently grouped into those present when a stationary, isolated airfoil is immersed in a uniform stream and those associated with blade rotation and inter-blade effects. The potentially important sources of noise for an isolated airfoil are; 1) vortex shedding, 2) incident turbulence, 3) the turbulent boundary layer, and 4) wake generated noise.

Vortex shedding is caused by interaction of the airfoil's wake-induced velocity field with the airfoil itself. The classic example of this mechanism is the Karman vortex street which occurs in a highly organized fashion in the wake of bluff bodies. The second noise mechanism[1,2] arises from random fluctuations in the turbulent velocity components incident on the airfoil which cause effective angle-of-attack changes, unsteady loads and hence noise. The third source is the turbulent boundary layer[3] which radiates noise directly and also produces edge noise, a mechanism arising from convection of turbulence past the sharp trailing edge. The fourth source is direct radiation from the turbulent wake.

Discrete frequency vortex shedding noise of vanes in water was clearly identified by Gongwer[4] who also related the frequency to a Strouhal number referenced to the sum of blunt trailing edge and turbulent boundary-layer thicknesses. Another study, however, found the relevant Strouhal number length scale for shedding to be the airfoil projection normal to the stream.[5] Sharland[1] conducted mea-

Presented as Paper 72-656 at the AIAA 5th Fluid and Plasma Dynamics Conference, Boston, Mass., June 26–28, 1972; submitted July 5, 1972; revision received February 21, 1973. The experimental study reported herein was funded by the Army Research Office, Durham, under Contract DAHCO4-69-C-0089. The authors wish to acknowledge the efforts of G. W. Johnston (presently of University of Toronto, Institute of Aerospace Sciences) and R. G. Schlegal (Sikorsky Aircraft) for their efforts in the initiation of the present study. Discussions with the latter and A. A. Peracchio and R. K. Amiet (UARL) during the course of the study were most helpful.

Index categories: Aerodynamic and Powerplant Noise (Including Sonic Boom); Aircraft Propulsion System Noise; Nonsteady Aerodynamics.

*Research Engineer, Aeroacoustics Group.

†Research Engineer, Aeroacoustics Group. Associate Member AIAA.

‡Senior Consulting Engineer, Aerodynamics. Associate Fellow AIAA.

§Acoustics Engineer.

surements of vortex shedding noise of an isolated airfoil at low Reynolds numbers and concluded that a) the acoustic intensity increased with velocity to the 5.6th power, b) the frequency spectrum was broadband relative to cylinder vortex shedding noise, c) the dominant frequency was determined by a Strouhal number of 0.2 referenced to airfoil thickness, and d) the surface pressure correlation lengths were on the order of half the section thickness. In other low-Reynolds number isolated-airfoil tests, Clark[6] obtained a velocity to the 6th power relation for noise intensity.

The present study was undertaken to determine vortex shedding characteristics for typical helicopter rotor sections at Reynolds numbers applicable to full-scale rotors through measurements of both surface and far-field acoustic pressures. The incident turbulence noise mechanism was suppressed relative to the vortex noise mechanism by conducting tests in an airstream of low turbulence level. To test the hypothesis that absolute airfoil thickness is the relevant length scale for vortex shedding noise, airfoils of two thicknesses were tested. To evaluate tip effects, a partial-span model was tested for comparison with a two-dimensional (full-span) model.

Initial results of this study, including an analytical formulation of discrete frequency airfoil vortex shedding noise, were given elsewhere.[7] An experimental study of the effect of leading-edge serrations on airfoil noise[8] was completed prior to and independently of that described here. It resulted in some similar observations and conclusions regarding airfoil vortex shedding.

Description of the Experiment

This study was conducted in the United Aircraft Research Labs. Acoustic Research Tunnel. The tunnel, shown schematically in Fig. 1, is a controlled turbulence level, open-jet wind tunnel designed specifically for aerodynamic noise research. For the present study the total turbulence level in the test section was approximately 0.1%. Far-field noise measurements were carried out in the quiescent region 7 ft above the test section centerline in the sealed anechoic chamber which surrounded the test section.

A rectangular test section 31 in. high, 21 in. wide, and 30 in. in length was chosen to provide two-dimensional flow test conditions. To obtain a uniform spanwise loading on the full-span airfoil models, the vertical sides of the jet were closed with sideplates extending from the contraction outlet into the jet collector. The use of sideplates eliminated the need to extend an airfoil or airfoil support through the thick, highly turbulent jet shear regions which would exist in their absence. Fluctuating airloads induced by these regions are a source of extraneous noise which cannot be evaluated unequivocably and which has existed in most isolated-airfoil studies.[1,6]

Three 9-in. chord models were tested in this study. Two of the models spanned the test section width (NACA 0012

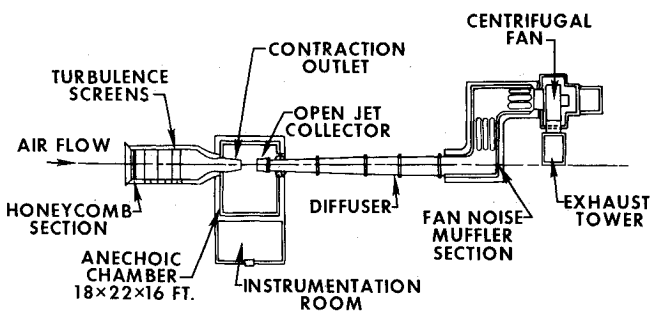

Fig. 1 UARL acoustic research tunnel.

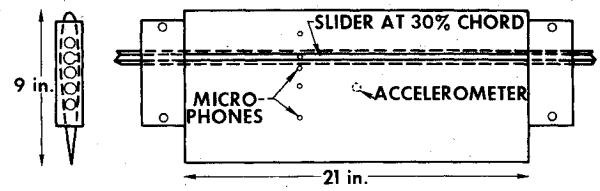

Fig. 2 NACA 0012 full-span airfoil.

and NACA 0018 sections). The third model had a NACA 0012 section and spanned half the test section width. To permit measurement of the local fluctuating surface pressure in both the span and chord directions, an array of ¼-in.-diam flush-mounted microphones was provided for each airfoil as shown in Fig. 2 for the full-span NACA 0012 airfoil. The tests were conducted with the microphone grids removed and the microphone diaphragms flush with the airfoil surface. Four microphones were fixed at one-third the test section span and 15, 38, 50, and 70% chord. The fifth microphone was mounted at 30% chord in a slider capable of traversing the model span. Microphone locations of 5, 30, 38, 70, and 80% chord were used for NACA 0018 model tests with the 30 and 70% chord microphones installed in sliders. Each model contained an accelerometer for vibration measurements. All listed angles of attack are geometric angles, which require a negative correction[9] to compensate for streamline curvature of the two-dimensional open jet. Far-field acoustic pressure fluctuations (Sound Pressure Level) and airfoil surface pressure fluctuations (Surface Pressure Level) are presented as 10 times the logarithm to the base 10 of the mean square unsteady pressure referenced to 0.0002 microbar. Additional details concerning the experimental arrangement are given elsewhere.[10]

Experimental Results

Vortex Shedding Noise Regimes

Initial tests conducted with the NACA 0012 full-span model produced several results which brought into question some previous assumptions[1] regarding vortex shedding noise of streamlined bodies. Figure 3 shows typical third-octave and 10 Hz far-field spectra obtained at Reynolds numbers of 8×10^5 and 2.2×10^6 for 6° angle of attack. At low Reynolds numbers such as 8×10^5 and moderate angles of attack, the far-field spectra were dominated by a strong signal in a single third-octave frequency band. Analysis with a 10 Hz bandwidth swept filter showed that the third-octave spike was because of one or more discrete-frequency tones. The tone frequencies were an order of magnitude higher than those corresponding to a Strouhal number of 0.2 referenced to airfoil thickness or projected thickness normal to the stream. A hot wire placed downstream of the airfoil trailing edge showed high-intensity wake fluctuations at the far-field dominant tone frequency. At higher Reynolds numbers such as 2.2×10^6, the airfoil noise could not be detected above tunnel background noise. The small increase of noise level over the tunnel-empty background level is attributed to increased jet collector background noise because of deflection of the airstream by the lifting airfoil. This conclusion is based upon an experimental study of the effect of open jet deflection on tunnel background noise in the absence of an airfoil which is discussed elsewhere.[11] Figure 3 shows that an increase of freestream velocity by a factor of 2.7 did not cause the 26 dB increase expected for a velocity to the 6th power vortex-shedding scaling law.

The result of a study of far-field noise spectra of the full-span NACA 0012 airfoil as a function of angle of at-

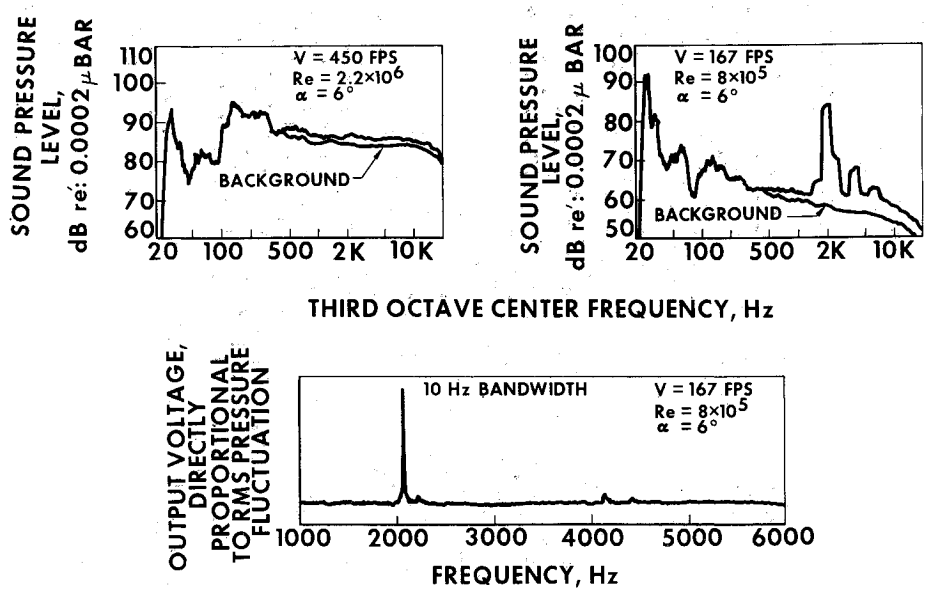

Fig. 3 Effect of Reynolds number on far-field spectra, NACA 0012 full-span airfoil.

tack and Reynolds number is shown in Fig. 4. Solid circles represent test points in the angle-of-attack velocity plane where vortex shedding noise was observed in third-octave far-field spectra. Numbers above the solid circles give the Sound Pressure Level of the dominant third-octave frequency band. Crosses denote test points at which the airfoil noise could not be detected above background.

Figure 4 shows that the α, V region in which vortex shedding noise was detectable above background noise was significantly larger for positive than for negative angles of attack even though the airfoil section was nominally symmetrical. Second, the velocity range over which vortex shedding noise was observed increased with angle of attack until the angle of attack reached values at which airfoil stall would be expected. Third, for a given positive angle of attack, the intensity of the tone increased with velocity for low velocities, reached a plateau or maximum, and then decreased with further increases in velocity prior to becoming undetectable. The regions of increasing or

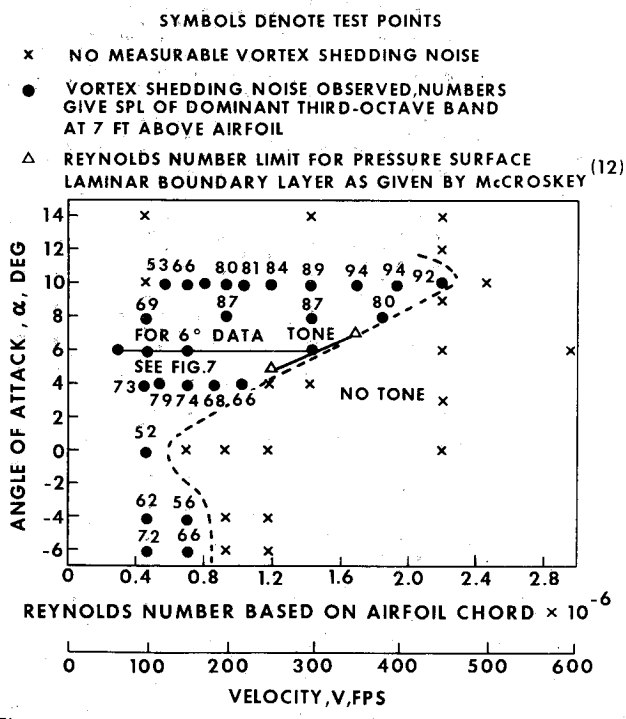

Fig. 4 Vortex shedding noise regimes, NACA 0012 full-span airfoil.

constant tone amplitude, decreasing tone amplitude and undetectable vortex noise are referred to herein as the tone, transition, and no-tone regimes, respectively.

A boundary-layer trip wire was found to have no effect on the tone when placed at various chord-wise positions on the suction surface of this airfoil but caused the tone to disappear when placed forward of 80% chord on the pressure surface. From this it was inferred that the presence of the tone was associated with a laminar boundary layer on the airfoil pressure surface. (Similar boundary-layer trip experiments and conclusions are reported by Hersh and Hayden.[8])

Based on the preceding hypothesis, the results of Fig. 4 can be explained. The velocity range over which vortex shedding noise was observed increased with angle of attack as the pressure gradient on the pressure surface became more favorable and the pressure surface boundary layer remained laminar over the full chord to higher Reynolds numbers. In fact, the angles of attack required for the pressure surface boundary layer to remain laminar to the trailing edge correspond closely to the dividing line between the tone and no-tone regimes. (The data of McCroskey[12] shows pressure surface transition occurring between 4 and 6° at $Re = 1.2 \times 10^6$ and 6 and 8° at $Re = 1.7 \times 10^6$. These points are shown as triangles in Fig. 4.)

The reason the α, V region in which the tone existed was smaller for negative than for positive angles of attack was that for negative angles of attack the slider at 30% chord was located on the pressure surface. The resulting small surface discontinuity served to trip the boundary layer from laminar to turbulent. Since the height of the slider discontinuity varied from 0.001 to 0.005 in. along the span, the pressure-surface boundary layer was laminar over restricted spanwise regions as compared to the full span for positive angles of attack. The tone amplitude would be expected to be proportional to the spanwise extent of laminar flow, and therefore was reduced.

Vortex Tone Regime—NACA 0012 Full-Span Airfoil

The noise measured in the tone regime qualitatively resembled discrete-frequency vortex shedding noise normally associated with bluff bodies. Since the presence of a laminar boundary layer on the airfoil pressure surface appeared to be central to the existence of the tone, a Strouhal number of 0.2 (that associated with bluff body shedding) referenced to twice the laminar boundary-layer thickness at the airfoil trailing edge was taken as the rele-

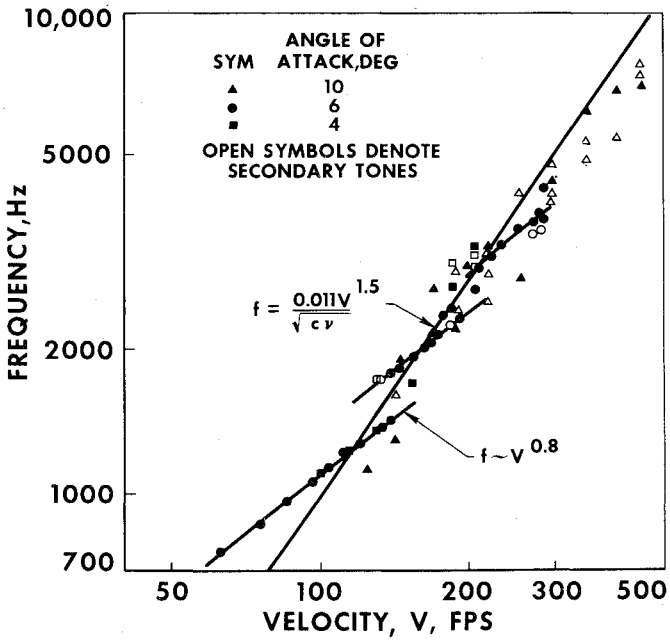

Fig. 5 Effect of velocity on far-field vortex shedding tone frequencies, NACA 0012 full-span airfoil.

vant nondimensional frequency scaling law

$$S = 0.2 = \frac{2f\delta}{V} \tag{1}$$

This assumption that the length scale was a characteristic dimension of the wake followed Roshko,[13] who postulated that the vortex shedding frequency must depend only on wake width and wake velocity. As a first approximation to the airfoil laminar boundary-layer thickness at the trailing edge, the result obtained for a flat plate (zero pressure gradient) was used

$$\delta = \frac{5c}{(Re)^{1/2}} \tag{2}$$

Substitution in Eq. (1) resulted in the following frequency scaling law

$$f = \frac{KV^{3/2}}{(c\nu)^{1/2}} \tag{3}$$

where K would have a value of 0.02 if the above numerical values were used. The frequency was, therefore, predicted to vary with velocity to the $\frac{3}{2}$ power (as opposed to the first power which applies to bluff bodies) and chord and kinematic viscosity to the $-\frac{1}{2}$ power.

Shown in Fig. 5 is a plot of the dominant tone frequencies (solid symbols) as a function of velocity at several angles of attack, determined by 10 Hz bandwidth analyses. The frequency dependence on velocity to the $\frac{3}{2}$ power is generally confirmed for the main trend of the data but not for the ladder-type behavior which comprises the trend. The major line shown in Fig. 5 is a plot of Eq. (3) with the constant, K, chosen as 0.011 to provide the best general fit of the data. This value corresponds to a Strouhal number of 0.11.

Several features of these data are of interest. First, the three lines showing the finer-grain trend for 6° angle-of-attack follow a frequency dependence on velocity to the 0.8 power. Second, at some velocities more than one discrete tone was apparent. For example, at 138 and 283 fps the two solid circles denote the presence of two discrete tones of approximately equal amplitude but differing frequency. Open circles at other velocities indicate the existence of secondary tones of lesser amplitude than the dominant tone. These secondary tones have been plotted only if their amplitude was within 10 dB of the dominant tone.

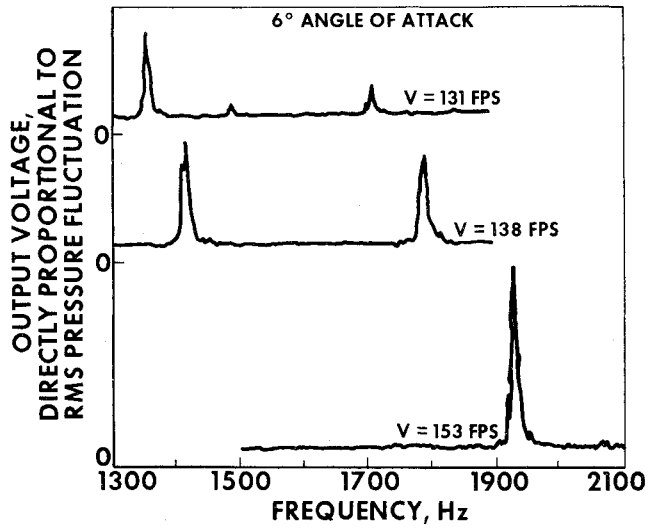

Fig. 6 Far-field spectra, NACA 0012 full-span airfoil at 10 Hz bandwidth.

Third, small increases in velocity generally resulted in a frequency dependence on velocity to the 0.8 power but occasionally caused a jump in frequency to the next highest 0.8 power line.

This dual tone behavior in the vicinity of 130 fps is shown in more detail in Fig. 6. As the velocity was increased from 131 to 138 fps the dominant and secondary tones increased in frequency proportional to velocity raised to the 0.8 power with the secondary tone growing in amplitude to approximately equal that of the once dominant tone. A further increase in velocity to 153 fps resulted in the disappearance of this once dominant tone and adherence to the 0.8-power frequency scaling by the new dominant tone. The reasons for the adherence to the 0.8 power frequency scaling law, the multiplicity of tones, and the apparent discrete jumps in frequency are at present unknown. Calculated cross duct resonance frequencies and airfoil transverse vibration frequencies do not correspond to the multiple tone and jump frequencies, nor can either mechanism account for the continuous dependence of the tones on velocity to the 0.8 power. It is therefore suggested that the origin of the jumps, multiple tones, and power dependence is aerodynamic in nature.

Figure 7 is a plot of far-field dominant tone amplitudes as a function of velocity for 6° angle of attack. It is apparent that the far-field tone amplitude increased rapidly with velocity for low velocities (possibly with the classical velocity to the sixth-power dependence) and fell off more rapidly at the end of the plateau. The relatively low amplitude observed at 131 and 138 fps is believed due to the presence of multiple tones. While only single tones were

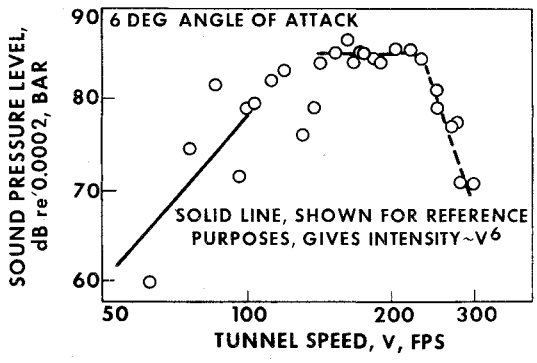

Fig. 7 Effect of velocity on far-field intensity at the tone frequency, NACA 0012 full-span airfoil.

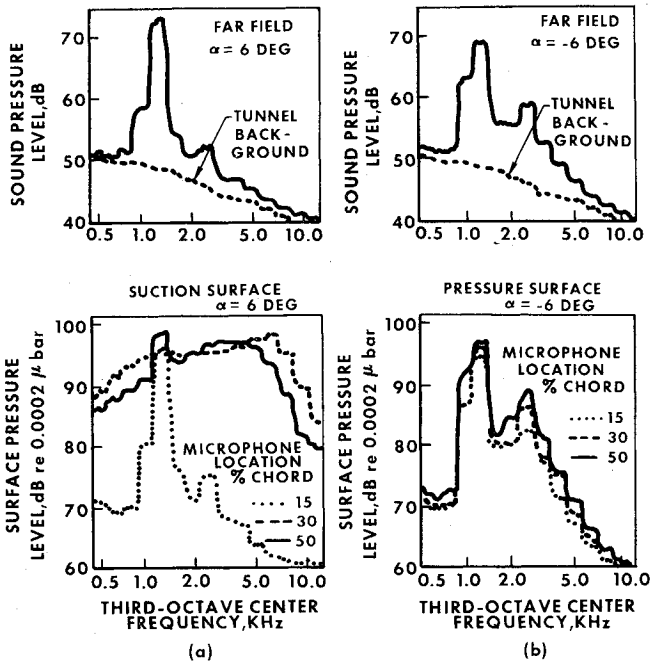

Fig. 8 Far-field and airfoil surface spectra for positive and negative angles of attack, NACA 0012 semispan airfoil.

found at the adjacent higher and lower velocities, multiple tones existed at these velocities. The existence of multiple tones, it is believed, is a manifestation of the loss of spanwise correlation relative to the single tone condition. Reduced correlation, in turn, could have caused the observed decrease in far-field amplitude.

For surface microphones located in a region of the airfoil for which the boundary layer was laminar, 10 Hz analyses of surface pressure microphones showed a strong signal at the same frequency for which a strong far-field signal existed. The general trend was for the intensity of this tone to increase in the downstream direction. Figure 8a gives both far-field and chordwise surface pressure spectra on the suction surface for the NACA 0012 semispan airfoil at an angle of attack of +6° and a tunnel speed of 100 fps. At 15% chord the boundary layer was laminar as evidenced by the low-amplitude pressure fluctuations at frequencies other than the tone frequency, whereas at 30 and 50% chord the boundary layer was turbulent. Figure 8b shows corresponding spectra for the airfoil at −6° for which the microphones were on the pressure surface. In this case the boundary layer remained laminar at all three microphone locations. The levels at the tone frequency were somewhat lower for the negative angle of attack because of the presence of the slider discontinuities on the pressure surface. Figure 8 therefore confirms the presence of a laminar boundary layer on the pressure surface during discrete-frequency vortex shedding. Surface pressure fluctuation measurements are reported elsewhere[10] in more detail.

Cross correlation between a microphone located 33.5 in. above the trailing edge, and a similar microphone located an equal distance below the model was carried out at an operating condition for which the airfoil produced a strong 1140 Hz vortex shedding tone. The cross correlation function was sinusoidal at a frequency of 1140 Hz with the cross correlation shifted 180° in phase angle with respect to the two sinusoidal autocorrelation functions. From this result it was inferred that the measured noise was of a dipole nature as would be anticipated for vortex shedding noise (Sharland[1]).

Figure 9 shows a typical surface pressure correlation in the tone region. The cross correlation coefficient (arrived at by normalizing the cross correlation sine wave amplitude by the product of the square root of the autocorrelation amplitudes measured at delay time greater than 0.5 msec) was approximately 0.9. Spanwise correlations between the fixed 38% chord and movable 30% chord microphone produced correlation coefficients of approximately unity for separation distances from 0 to 8 in. in span. These measurements demonstrate that the pressure fluctuations in the tone regime are coherent over a considerable extent of the model surface.

The delay time increment in Fig. 9 between the peaks of the autocorrelation and cross correlation, measured to be 260 ± 25 μsec, indicated that the correlated pressure signal arrived at the 30% chord microphone this increment in delay time later than at the 70% microphone. Based on the microphone spacing, the correlated pressure signal traveled forward along the airfoil at a speed between 1040 and 1240 fps which is close to the speed of sound. Measured delay time increments for other microphones confirmed this result suggesting that the origin of the pressure disturbance was near the trailing edge as

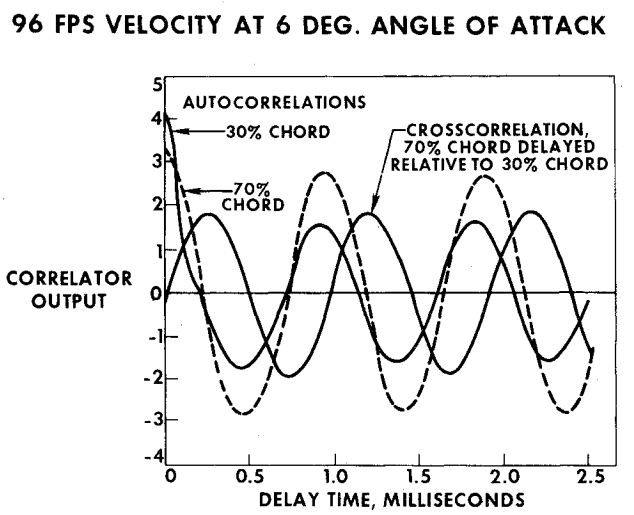

Fig. 9 Typical surface pressure correlations in the vortex tone regime, NACA 0012 full-span airfoil.

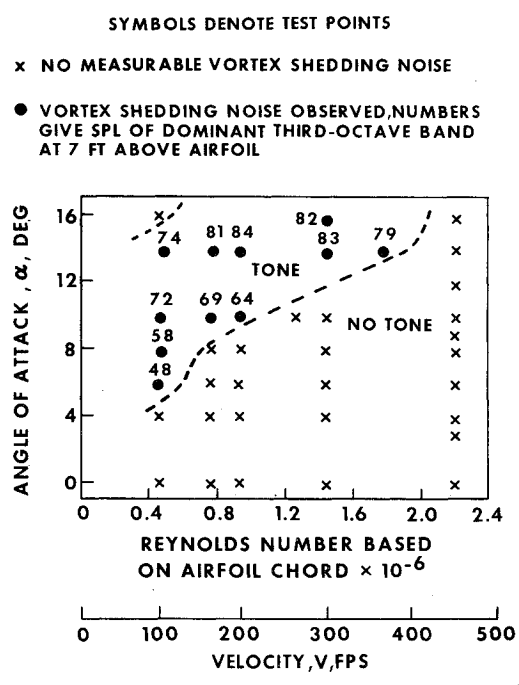

Fig. 10 Vortex shedding noise regimes, NACA 0018 airfoil.

would be anticipated for a wake-dominated phenomenon. This result also means that the phase angle is a function of chordwise position on the airfoil. Surface and far-field pressures also were found to be highly correlated at the tone frequency.

While acceleration measurements of the airfoil showed a dominant frequency spike at the far-field tone frequency, the corresponding displacement was several orders of magnitude smaller than the airfoil boundary-layer displacement thickness at the trailing edge. Based on these results, the airfoils could be considered to be rigid in this study.

Effect of Airfoil Thickness and Finite Span on the Tone Regime

If the relevant dimension for vortex shedding noise were airfoil thickness as used by Sharland[1] and by Hersh and Hayden,[8] the primary effect of a change from an NACA 0012 to an NACA 0018 section of equal chord would be a decrease in frequency of the vortex shedding noise by a factor of 1.5. If laminar boundary-layer thickness at the trailing edge were the relevant length scale, then the effect of airfoil thickness ratio on frequency would be expected to be minimal. The principal effects would be expected to occur in the region of the angle of attack velocity plane over which shedding noise was observed.

The results shown in Figs. 10 and 11 confirm that laminar boundary-layer thickness rather than absolute airfoil thickness is the controlling length scale. The frequencies for the full-span NACA 0018 at 10° angle of attack, shown in Fig. 11, agree quite well with the corresponding full-span NACA 0012 data given in Fig. 5. In addition, the extent of the tone regime shown in Fig. 10 is displaced upward in angle of attack relative to the tone regime for the NACA 0012 full-span airfoil shown in Fig. 4. This is consistent with the expected effect of increased section thickness on the minimum angle of attack for which the pressure surface boundary layer is laminar to the trailing edge. The existence of the tone at higher angles of attack than for the NACA 0012 full-span airfoil is consistent with the expected delay in stall to higher angles of attack due to increased thickness at these test Reynolds numbers. These results support the contention that the tone does not exist when the airfoil is fully stalled from the leading edge.

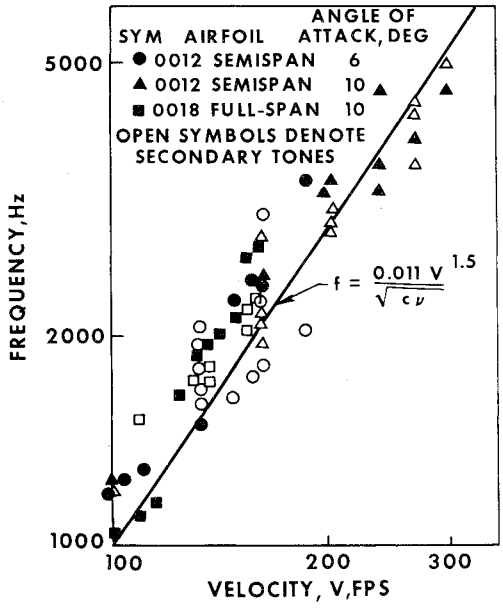

Fig. 11 Effect of velocity on far-field vortex shedding tone frequencies, NACA 0018 and semispan NACA 0012 airfoils.

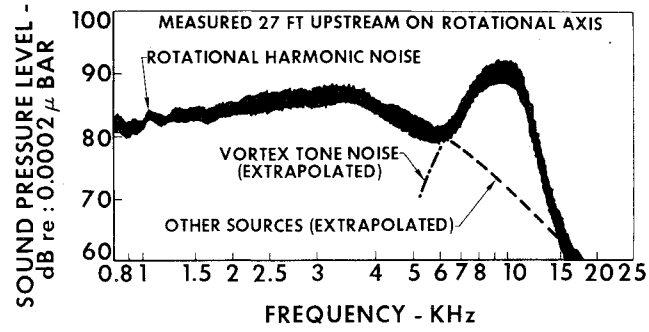

Fig. 12 Full-scale tail rotor noise spectrum, 8% bandwidth analysis, 3° collective pitch.

As shown in Fig. 11, the vortex shedding tone frequencies for the semispan NACA 0012 model were similar to those obtained with the full-span models. For low angles of attack the tone regime was displaced some 2×10^5 downward in Reynolds number relative to Fig. 4 for the full-span model.[10] The primary difference, however, was that the tone regime for the semispan model extended to significantly higher angles of attack than for the full-span model. This is believed to be caused by the decrease in effective angle of attack associated with the potential flowfield of the tip vortex which results in the delay of stall to higher geometric angles of attack. In general, vortex shedding noise was not appreciably altered by the semispan model's tip vortex.

Transition and No-Tone Regimes

The transition regime has been defined as the restricted range in Reynolds number over which the far-field tone amplitude decreased with increasing Reynolds number prior to becoming undetectable above tunnel background. Simultaneous measurements of the far-field noise and surface pressure fluctuations demonstrated[10] that decay of the tone in the transition regime was associated with gradual turbulent transition of the pressure-surface boundary layer. The details of the transition regime are at present unknown; however, it appears that both the magnitude of surface pressure fluctuations and the correlation length at the tone frequency decrease as Reynolds number increases, presumably because of increased spanwise extents of turbulent flow at the trailing edge.

A basic finding of the present study is that at high Reynolds numbers, vortex shedding noise from streamlined airfoils is not evident in the far-field spectra. While it cannot be proven that vortex shedding noise disappears at high Reynolds numbers, it can be stated that vortex shedding noise, if it exists, is lower in intensity than the relatively low tunnel background noise, and, therefore would be a relatively weak noise source. This is evident from Fig. 3 which shows a tunnel background noise spectrum in the no-tone regime. Further confirmation of the lack of vortex shedding noise at high Reynolds number was obtained from the measurements of the airfoil surface pressures. The behavior was characteristic of turbulent boundary layer pressure fluctuations. That is, the surface pressure fluctuations at low angles of attack were on the order of 0.5% of the freestream dynamic pressure which is a typical magnitude for turbulent boundary layers.[14] In addition, cross correlation of surface pressures showed that the pressure fluctuations were convected downstream at a velocity of 83% of the freestream velocity at a Reynolds number of 2.2×10^6. This is the same value obtained[14] for downstream convection of low-frequency eddies in a turbulent boundary layer.

Cross correlations were conducted with the NACA 0018 airfoil between the fixed 80% chord microphone and the

70% microphone traversed in span, at a Reynolds number of 2.2×10^6 and 6° angle of attack. At this no-tone condition, the cross correlation coefficient for spanwise separations of ½ in. and greater was zero. This means that the spanwise correlation length of vortex shedding, if shedding existed, was smaller than ½ in. For flat-plate turbulent boundary layers, the correlation lengths have been determined[14] to be on the order of the boundary-layer displacement thickness. The displacement thickness at 80% chord would be expected to be somewhat greater than 0.02 in. Because of the relatively large size of the surface pressure microphone diaphragms (0.234 in.), it was not possible to prove that the spanwise correlation length was typical of values obtained for turbulent boundary layers. Also, the microphones were located too far from the trailing edge to assess the turbulent boundary-layer "edge noise" mechanism. It was therefore, not possible to conclude whether the far-field amplitude of vortex shedding noise in the no-tone regime (if such noise existed) was lower than that due to the turbulent boundary layer.

The lack of detectable vortex shedding at high Reynolds numbers suggests that the interaction of two adjacent turbulent boundary layers of opposite vorticity does not lead to correlated vortex shedding. This conclusion would be expected to be valid for other airfoil sections, operating unstalled, except in cases where a blunt trailing edge provided significant bluff-body spacing between the two boundary layers at the trailing edge. It is not known why the presence of one laminar boundary layer is critical to the phenomenon. Presumably it allows the wake sufficient time to concentrate vorticity by inviscid flow interaction between the upper and lower boundary layers before diffusion and convection of vorticity by turbulent components cause vorticity cancellation.

Comparison With Other Data

Clark[6] obtained far-field acoustic spectra for both cambered and uncambered NACA 65 series airfoils of 10% thickness ratio and 2-in. chord. The velocity dependence of far-field peak frequencies, given in his Figs. 14 and 15, is correlated fairly well by Eq. (3) with K taken equal to 0.011 (that obtained from Fig. 5 above). Smith et al.[15] give far-field third-octave spectra for low altitude sailplane flybys. The spectrum for a Libelle sailplane at 104 fps from their Fig. 66 shows a strong tone in the 1000 Hz third-octave band. Based on the tip chord of about 13 in., Eq. (3) would predict a vortex shedding tone at 900 Hz.

Hersh and Hayden[8] reported that pure tones were generated by a 6-in.-chord NACA 0012 airfoil at third-octave center frequencies of 800 and 1600 Hz for velocities of 60 and 100 fps, respectively. These tones are similar to those reported here. Using Eq. (3) and NACA 0012 full-span tone frequencies (Fig. 5) tones for the 6-in.-chord airfoil would be predicted to occur at 875 and 1320 Hz for the referenced velocities, values close to the reported third-octave band frequencies. The same study also reported that a 2-in.-chord, 14-in.-diam, two-bladed NACA 0012 model propeller produced tones in the 3150 or 4000 Hz third-octave band at 2000 rpm and 8000 Hz band at 4000 rpm which dominated the noise spectrum. Based on the velocity at the propeller tip for these two cases (130 and 250 fps), Eq. (3) and Fig. 5 would predict vortex shedding tones at 3200 and 8500 Hz for the two rotational speeds, values in close agreement with those reported.

To determine the relevance of the present study to helicopter rotors, noise measurements were examined, during this study, for a full-scale helicopter tail rotor operating at design rpm on a rotor whirl test stand. The rotor was an untwisted 5-bladed, 10.3-ft-diam., 0.61-ft-chord Sikorsky tail rotor with a modified NACA 0012 section. Figure 12 shows a typical spectrum measured on the rotational axis at 1243 rpm and 3° blade geometric collective pitch angle. Using Eq. (3) the expected frequency range for vortex shedding tones would be predicted to be between 2 and 19 KHz corresponding to the root and tip velocities of the blade, respectively. Figure 12 shows a broadband hump over the frequency range from 7 to 15 KHz which is within the predicted vortex tone noise range. Based on a more detailed analysis of tail rotor spectra, it was concluded[10] that the effect of rotation was to alter the angle of attack Reynolds number range over which strong vortex shedding tone noise occurred. This was attributed to the effect of rotation on pressure-surface turbulent transition and the yet unexplored but presumably important effect of spanwise velocity variation on spanwise vortex shedding correlation lengths.

References

[1]Sharland, I. J., "Sources of Noise in Axial Flow Fans," *Journal of Sound and Vibration*, Vol. I, No. 3, 1964, pp. 302–322.

[2]Dean, L. W., "Broadband Noise Generation by Airfoils in Turbulent Flow," AIAA Paper 71-587, Annapolis, Md., 1971.

[3]Powell, A., "On the Aerodynamic Noise of a Rigid Flat Plate Moving at Zero Incidence," *Journal of the Acoustical Society of America*, Vol. 31, No. 12, Dec. 1959, pp. 1649–1653.

[4]Gongwer, C. A., "A Study of Vanes Singing in Water," *Journal of Applied Mechanics*, Vol. 19, No. 4, Dec. 1952, pp. 432–438.

[5]Krzywoblocki, M. Z., "Investigation of the Wing-Wake Frequency With Application of the Strouhal Number," *Journal of the Aeronautical Sciences*, Vol. 12, No. 1, Jan. 1945, pp. 51–62.

[6]Clark, L. T., "The Radiation of Sound From an Airfoil Immersed in a Laminar Flow," *Transactions of the ASME, Journal of Engineering for Power*, Vol. 93, Ser. A, No. 4, Oct. 1971, pp. 366–376.

[7]Paterson, R. W., Vogt, P. G., Amiet, R. K., and Fink, M. R., "Vortex Shedding Noise of an Isolated Airfoil," *Proceedings of the Helicopter Noise Symposium*, U.S. Army Research Office, Durham and American Helicopter Society Inc., Sept. 28–30, 1971, Durham, N.C., pp. 73–83.

[8]Hersh, A. S. and Hayden, R. E., "Aerodynamic Sound Radiation from Lifting Surfaces With and Without Leading Edge Serrations," Contractor Rept. CR-114370, June 1971, NASA.

[9]Pope, A. and Harper, J. J., *Low-Speed Wind Tunnel Testing*, Wiley, New York, 1966, p. 316.

[10]Paterson, R. W., Vogt, P. G., Fink, M. R., and Munch, C. L., "Vortex Shedding Noise of an Isolated Airfoil." Rept. K910867-6, Dec. 1971, United Aircraft Research Labs., East Hartford, Conn.

[11]Paterson, R. W., Vogt, P. G., and Foley, W. M., "Design and Development of the UARL Acoustic Research Tunnel," AIAA Paper 72-1005, Palo Alto, Calif., 1972; also *Journal of Aircraft*, to be published.

[12]McCroskey, W. J., "Measurement of Boundary Layer Transition, Separation and Streamline Direction on Rotating Blades," TN D-6321, April 1971, NASA.

[13]Roshko, A., "On the Wake and Drag of Bluff Bodies," *Journal of the Aeronautical Sciences*, Vol. 22, No. 2, Feb. 1955, pp. 124–130.

[14]Willmarth, W. W. and Wooldridge, C. E., "Measurements of the Fluctuating Pressure at the Wall Beneath a Thick Turbulent Boundary Layer," *Journal of Fluid Mechanics*, Vol. 14, Pt. 2, Oct. 1962, pp. 187–210.

[15]Smith, D. L., Paxson, R. P., Talmadge, R. D., and Hotzo, E. R., "Measurements of the Radiated Noise from Sailplanes," TM-70-3-FDAA, July 1970, U.S. Air Force Flight Dynamics Lab., Wright-Patterson Air Force Base, Ohio.